Anal. Bioanal. Electrochem., Vol. 12, No. 5, 2020, 712-732

Analytical& Bioanalytical Electrochemistry

2020 by CEE
www.abechem.com

Full Paper

Development of a Disposable Electrochemical Sensor based on Nanocomposite/Ionic Liquid Assisted Hollow Fiber-Graphite Electrode for Measurement of Lorazepam Using Central Composite Design

Mohammad Vahidifar,* and Zarrin Es'haghi*

**Department of chemistry, Payame Noor University, 19395-4697 Tehran, Iran*

*Corresponding Author, Tel.: +98 51 38683004-118

E-Mail: zarrineshaghi@gmail.com; eshaghi@pnu.ac.ir

Received: 1 April 2020 / Received in revised form: 20 May 2020 /
Accepted: 22 May 2020 / Published online: 31 May 2020

Abstract- In this study a new method of preconcentration, separation and efficient measuring of so-called hollow fiber solid / liquid phase microextraction has been introduced for the determination of trace amounts of lorazepam (LRZ) in water samples, urine and hair using differential pulse voltammetry. To this end, a hybrid adsorbent material was used that involved ionic liquid assisted magnetic multi-walled carbon nanotube as the extraction phase. Nanoparticles dispersed in the ionic liquid were placed inside the pores and channels of hollow polypropylene fiber. Then the pencil graphite electrode modified with multi-walled carbon nanoparticles was put into this fiber. This combined electrode was placed in a voltammetry cell and use as a working electrode. The electrochemical behavior of LRZ on the fabricated working electrode was investigated by differential pulse voltammetry (DPV) techniques and the obtained results confirmed its efficiency for sensing of LRZ. The study was approved using the Placktett-Burman design (PBD) for screening and central composite design (CCD) for the optimization of the process parameters. Under optimal conditions, a linear calibration curve was plotted for the concentration of analyte between 0.032 to 64.2 µM with a detection limit (LOD) (S/N=3) and limit of quantification (LOQ) of 0.003 µM and 0.06 µM respectively. The suggested method was successfully applied for screening real samples; domestic water, urine and hair for LRZ.

Keywords- Lorazepam; Hollow fiber solid/ liquid phase microextraction; Differential pulse voltammetry; Central composite design

1. INTRODUCTION

Benzodiazepines (BZPs), are heterocycles containing a benzene ring of seven members, including two hetero-nitrogen atoms that are based on the position of the placement of the nitrogen (relative to each other). They are divided in to two major groups of 1,4-benzodiazepines and 1,5- benzodiazepine. High biological activity found in benzodiazepines and the introduction of chlordiazepoxide (the first, 1,4-benzodiazepine having significant anti-anxiety and anti-spasm features) in 1960 became a turning point in the pharmaceutical industry, as human life in the late 20th century and the beginning of 21st century has been filled with stress and anxiety and there is a growing need of medication which can free them from this pressure. Benzodiazepines have a high usage in Pharmacology by increasing Gamma Amino butyric acid neurotransmitter and by having anticonvulsant, anesthetic, antidepressant, hypnotic and sedative properties [1]. They are also used as a pre-drug to induce general anaesthetization applications, and are thus widely prescribed worldwide [2]. Benzodiazepines are active intermediaries over a long period of time. The short period effects of benzodiazepines are favoured in the treatment of insomnia and their long effects are suggested for the treatment of anxiety [3]. However, many cases of drug poisoning and one of the important factors in driving accidents, as a result of sedation-dizziness, have been the use of benzodiazepines. Due to the double-effect of these compounds, they have been successful in the treatment of seizure, anxiety and insomnia, and have also because of a higher degree of certainty, been able to take the pace of barbiturates, and have become one of the most widely used medications for humans [4,5] and animals [6]. The most popular drugs in this category are: alprazolam, diazepam, clonazepam, oxazepam, lorazepam and chlorodiazepoxide. Needless to say, because of the above properties, they have also been used by criminals to disable victims. The determination of benzodiazepines has been extensively investigated because of the need to identify and measure them quantitatively in clinical and forensic studies. The decomposition of these compounds is one of the important parts of many pharmaceutical decomposition laboratories. Lorazepam with formula $C_{15}H_{10}Cl_2N_2O_2$ (Fig. S1) is one of the most commonly used drugs of the benzodiazepine family. It is prescribed to reduce symptoms of anxiety, sleep and phobia disturbances; plus, it is also used as a muscle relaxant.

Most widely used techniques include high-performance liquid chromatography (HPLC) [7-9], gas chromatography–mass spectrometry (GC-MS) [10-12], liquid chromatography-mass spectrometry (LC-MS) [13-23], have been used to the benzodiazepines and their metabolites assay in biological fluids. Meanwhile, electrochemical methods (as fast, simple, inexpensive systems with high selectivity and repeatable results) have a special place. A wide range of eco-friendly electrochemical sensors that meet these needs are commercially available.

Different electrodes, such as the dropping mercury electrode (DME), and the glassy carbon electrode (GCE) have commonly been used to measure different analytes [24].Various sample preparation methods have also been used for clean-up and preconcentration of the analytes in aqueous media. Among the existing methods, liquid-liquid extraction (LLE), solid phase extraction (SPE) [25,26] and other liquid phase microextraction (LPME) [27], have been developed for this purpose. Among these methods, Solid Phase Microextraction (SPME) is one of the most important techniques. Although, SPME fibers are expensive and have a brittle and delicate coating that must be used with care. In addition, the number of coatings used in SPME is limited, molecular weight can be absorbed at the fiber surface and there is a possibility for earlier tests to affect following experiments [28]. Therefore, in some cases, it is better to use a modified method called hollow fiber solid/liquid phase microextraction (HF-SLPME), which was first introduced by Zarrin Es'haghi, et al [29]. Thus, this study was undergone to promote the SPME method by placing nanoparticles into the polypropylene hollow fiber pores through an appropriate solvent or ionic liquid (IL) as a solid/liquid absorbent. According to this idea, the membrane which is activated by nanoparticles acts as a trap with higher enrichment and selectivity. Results displayed a significant development compared to the typical hollow fiber LPME [30].In this work, the hollow fiber micro-solid/liquid phase extraction was coupled to an electrochemical technique. In this method, the character of an intermediate solvent is also important because the polypropylen membrane must be compatible with the solvent and keep it in its pores. A solvent must be designated according to the fiber assembly so that it does not leave the fiber pores. In this case some green, chemical inert, non-flammable and stable liquids were used. A number of these solvents were tested, where ultimately; an ionic liquid, 1-Hexyl-3-methylimidazolium hexafluorophosphate was selected as the best solvent for further experiments [31].

The lorazepam presented to the hollow fiber pores is divided between the two phases, ionic liquid and magnetic multi-walled carbon nanotube (MWCNT-Fe_3O_4) nanocomposite. Ionic liquid-based HF-SLPME has numerous advantages over traditional methods, such as extra protection, being ecologically friendly and high preconcentration factors. The selected ionic liquid that was placed in the fiber pores, acting as a liquid trap and one of the acceptor phases along with the nanocomposite system. The analyte molecules were extracted into the hollow fiber membrane through intermolecular and diffusion forces.

An electrical contact was established through pencil graphite which was placed within the fiber. The disposable nature of fiber electrodes leads to reduce interference, the easy preparation process, low background currents, the high sensitivity and stability, and practical potential for the construction of new sensors for many important species.

In this method, a solid adsorbent of MWCNT-Fe_3O_4, which was completely spread in ionic liquid ([HMIM][PF_6]), and placed within the fiber-wall cavities, was used as an

extraction agent. Then, extraction, purification and quantitative measurements were performed simultaneously with applying differential pulse voltammetry technique (DPV).

The Central Composite Design Method (CCD) was done to obtain optimal experimental conditions, and used main parameters to assess the effects on electrochemical response. Compared to other chemometrics methods, CCD is a simple method and by reducing the number of experiments it can save test cost and time. Finally, in order to prove its efficacy, this electrochemical sensor was investigated for preconcentration and measurement of lorazepam in hair and water samples.

2. EXPERIMENTAL

2.1. Apparatus

All electrochemical measurements were done by means of potentiostat/galvanostat (SAMA 500, analyzer system, Iran). Voltammetry experiments were implemented in a three-electrode cell consisting of the Ag/AgCl reference electrode containing a saturated solution of potassium chloride and platinum wire auxiliary electrode while graphite electrode (PGE)/ hollow fiber was utilized as a working electrode. Pencil graphite with a diameter of 0.7 mm, grade HB hardness, manufactured by German Rotring Company was used. Medication voltammograms were obtained by the DPV method. Measuring and adjusting pH was done with a digital pH meter, (Model 827, Metrohm, Switzerland) equipped with an integrated electrode (calomel/glass electrode). The morphology and size of the nanoparticles and the structure of the hollow fiber and graphite electrode were investigated using a Hitachi SEM (SEM) S-4160 and Infrared Spectroscopy (FTIR) of Bruker tensor 12 made in Germany. The X-ray diffraction (XRD) crystallography test was used to characterize the phase formed and size of crystals using the PW1800 X-ray machine from Philips and the copper lamp to do this. The samples used for this test were in powder form. For synthesis of nanoparticles, a helmet-MK11 magnetic stirrer and a Binder-FD 13 vacuum oven were used. In all the experiments, the water which was used was double deionized water by a water purification plant manufactured by Aqua Max-Ultra Youngling (South Korea, Seoul). For magnetic separation, a neodymium magnet was used with a magnetic intensity of 1.3 Tesla.

2.2. Materials and Reagents

All materials used were prepared by Analytical rank. The drugs required in this study, lorazepam was supplied by Sobhan Drugs, and the chemicals: ($FeCl_3.6H_2O$), ($FeCl_2.4H_2O$), ammonia, the ionic liquids([BMIM]/[PF_6]),([OMIM][BF_4]), and ([HMIM][PF_6]), acetonitrile, N,N-dimethylformamide, octanol, methanol, acetone, ethanol, were acquired from Merck (Darmstadt, Germany) whereas sulfuric acid, nitric acid, hydrochloric acid, acetic acid, phosphoric acid, potassium dihydrogen phosphate and potassium hydroxide used in the

preparation of buffers were bought from Sigma-Aldrich. Multiwall carbon nanotubes with purity of 95% with an average external diameter of 20-30 nm, a length of 1-15 μm, and a number of walls of 3-15 were prepared from the Research Institute of the Oil Industry. Moreover, the necessary solutions were prepared and used daily. The hollow fiber polypropylene membranes with a specification of Accurel PP Q 3/2 and a wall thickness of 200 μm, an internal diameter of 600μm, pore size of 0.2 μm and the ~70% wall porosity were supplied by Membrana GmbH (Wuppertal, Germany). Hollow fiber was divided into 1.5 cm pieces. By placing these parts in acetone, the fibers were cleaned and dried before use. Phosphate buffer solutions were prepared by adding H_3PO_4 and KOH dilute solutions to 0.1 M solution of KH_2PO_4 salt (phosphate buffer) and acetate buffer solution by adding dilute KOH solution to molar acetic acid solution (acetate buffer) and the pH adjustment of the resulting solution was prepared with a pH meter. Medication base stock solution was arranged at a concentration of 500 μg/ml in methanol and kept at 4 ºC. Daily working solutions that were extracted from, through diluting the base solution with double distillation water, were prepared freshly every day.

2.3. Preparation of multi-walled carbon nanotube

For the purpose of activate the carbon nanotubes, first 100mL of 63.1% nitric acid was added to 10 g of multi-walled carbon nanotubes and sonicate for 15 minutes. This was done to increase the porosity and activation of the MWCNTs. With the intention of eliminate the acidity, the MWCNTs were washed with sufficient deionized water and dried in an oven at 70ºC for 4 hours and kept in sealed containers.

2.4. Synthesis of MWCNTs-Fe_3O_4

The co-precipitation method was used to construct magnetic nanoparticles [32]. Before adding reagents, 200 ml deionized water was exposed to the nitrogen gas in a multi aperture glass reactor and deoxygenated. Then 5.12 g of$FeCl_3.6H_2O$ and 2.00 g of $FeCl_2.4H_2O$ were added to the water. After that, the solution temperature gradually reached 80ºC. Then, a solution of ammonium (1.5 M) was added to the solution in the reactor droplet by droplet under the nitrogen atmosphere and stirring (600 rpm), to obtain the pH between 8 and 10.The solution was then stirred for two hours under the above-stated conditions. At this stage, black deposits formed, indicating the formation of Fe_3O_4 nanoparticles. The infrared spectra are shown in Fig. S2a, and the Fig. S2b and S2c, show XRD and SEM of the magnetite nanoparticles, respectively.

In conclusion, 50 mg of MWCNTs were added into the solution and the mixture was stirred for 30 min. Then, the mixture was heated (up to 35 ˚C), NH_4OH solution added drop wise until the pH was raised to 9. The mixture was agitated for 1 h. Later, the resulting black

sediment was stirred at 60 ˚C for 30 minutes. The whole process is done in the presence of nitrogen gas.

After cooling, the sample reached ambient temperature; the resulting sediment was separated by centrifugation and washed several times with deionized water and ethanol respectively. Lastly, the synthesized sorbent recovered, and dried in vacuum overnight at 40 ˚C.

The FTIR spectrum of Fe_3O_4 nanoparticles is shown in Fig. S2a. In this spectrum, the peak of 573 cm^{-1} is related to the Fe-O-Fe group and the observed peak of about 3380 cm^{-1} is related to the OH group.

Fig. S2b shows the x-ray diffraction patterns. These patterns indicate specific peaks at 2 θ values of 31, 36, 43, 54, 57 and 63, related to phases 220, 311, 400, 442, 440, and 550 of Fe_3O_4 nanoparticles, respectively. So, it can be concluded that Fe_3O_4 nanoparticles have been successfully fabricated.

The crystalline size of the nanoparticles has been estimated from the width of the highest peak in phase 311 using the Scherer equation. The resulting peaks are sharp and totally clear, representing the good crystallization and uniformity. No peaks connected to the impurities were observed, indicating a high purity of the prepared nanoparticles. An example of magnetized nanomagnetic particles images produced by the transmitted electron microscope (SEM) of the synthesized sample can be seen in Fig. S2c. As it is known, the particle sizes in the nanometer dimension are in the range of 43–66 nm, and the results show homogeneous spherical particles.

The symmetric and anti-symmetric C-H stretching motions are observed at frequencies of 2825.12 cm^{-1} and 2854.13 cm^{-1} and the C=C bond at a frequency of 1636.56 cm^{-1} found in oxidized nanotubes.

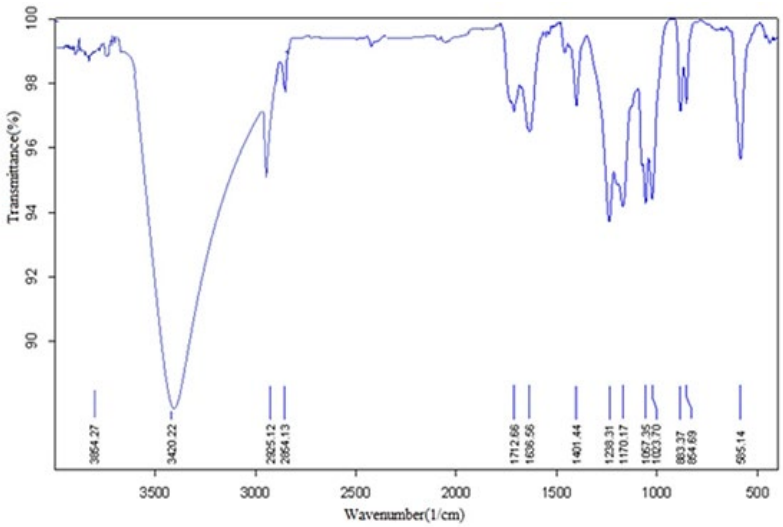

Fig. 1. FT-IR spectrum MWCNTs-Fe_3O_4

The wide peak of the O-H stretching motions at a frequency of 3420.22 cm^{-1} and a C=O peak at a frequency of 1712.66 cm^{-1}, which is related to the carbonyl group, has confirmed the oxidizing of the nanotubes. Fig. 1 shows oxidized carbon nanotubes.

2.5. Coating of magnetic multi-walled carbon nanotube with ionic liquid

To improve the surface of Fe_3O_4 nanoparticles with ionic liquid, 1.5 g of magnetic multi-walled carbon nanotube nanoparticles were slowly added to a solution containing 0.5 g of ionic liquid ([HMIM][PF_6]) in 15 mL of acetone while stirring. After stirring at room temperature for an hour, the solvent was evaporated and methylene chloride and deionized water used to wash the remaining solid. Then it was dried at 60°C for two hours and stored for further use. The infrared spectrum is shown in Figure S3a and the XRD spectrum, in Figure S3b. In order to study the phase structure of matter, the XRD pattern of nano-adsorbent compared with the standard powder diffraction cards issued by the Joint Committee on powder diffraction standers (JCPDS). As we can see, the peaks of the magnetite index are observed at angles of 30.0, 35.3, 9.24, 5.53, 9.56, and 62.5, which match the magnetite crystalline screens: (220), (311), (400), (422), (511), (440).

For further investigation of the nano-absorbent structure, FTIR spectra were used. The strong absorption bar in the 1580 cm^{-1} corresponds to the Fe-O magnetite bond. As a result of the ionic liquid connection, the infrared spectrum shows the picks of 3170 cm^{-1} and 3121 cm^{-1} stretching vibration of the CH imidazolium ring, 2980 cm^{-1} and 2936 cm^{-1} (stretching vibrations of -CH_3 and -CH_2, 2815 cm^{-1}) stretching vibration (N -CH_2, 1572 cm^{-1}) stretching vibration of CC and CN imidazolium ring) and 844cm^{-1} (stretching vibration of PF).

2.6. Preparation of PGEs before the surface modifying process

Prior to modifying the PGE surface with carbon nanotubes and in order to prepare the PGE, the electrode was first immersed in deionized water and ethanol repeatedly for clearing, and at each step has been located in an ultrasound bath for 5 minutes. The electrode surface was then activated by electrochemical method. The electrodes were placed in an electrochemical tubule containing 0.5 M acetate buffer solution at pH=4.8 and its surface was activated by applying a potential in the range of -1 volt to +4 volts for 500 s by cyclic voltammetry. After completion of the above operation, the respective electrode was totally washed with deionized water and used as an unmodified electrode in subsequent voltammetry studies.

2.7. Preparing modified PGE with magnetic multi-walled carbon nanotube

A suspension was prepared by adding 2 mg of magnetic functionalized multi-walled carbon nanotube in 5 mL of N, N-dimethylformamide (DMF) solvent under ultrasound waves

for 5 min that produced a suspension of black colour. In order to modify the surface of the pencil graphite functionalized electrode, it was placed sedentary in the modifier suspension for 5 hours and the surface modified electrode dried at room temperature for 12 hours (Scheme 1). Fig. 2a and Fig. 2b SEM spectrum of bare and carbon nanotubes modified PEGs was taken on a pencil graphite electrode.

2.8. Graphite-hollow fiber electrode fabrication

In the first stage, the hollow fiber polypropylene was cut into 2 cm pieces. To remove the impurities, the cut pieces were washed by acetone and dried in the open air. Then, ionic liquid was dissolved in a solvent of octanol (70:30), and due to study the effect of nanoparticles in the first experiment, 30 mg of magnetic multi-walled carbon nanotube, which had previously been operated by the same ionic liquid, were poured into the solution.

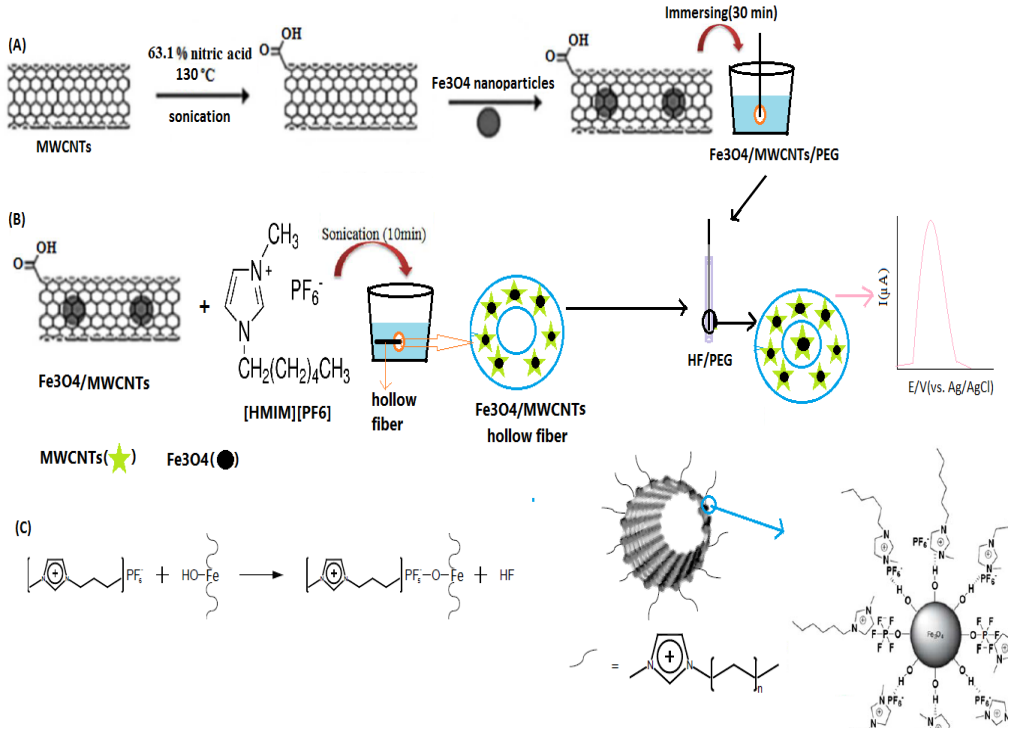

Scheme 1. Preparation of MMWCNTs/IL/HF-PGE

They were scattered by ultrasound waves. Prepared hollow fiber parts were thrown into the solution (including magnetite nanoparticles and ionic liquid) and mixed. In the second stage, 1.7 cm of pencil graphite modified with magnetic multi-walled carbon nanotube was placed within each hollow fiber cut cautiously. The open end of the fiber was blocked by heat. The fabricated graphite-hollow fiber electrode was then washed with deionized water and transferred to the voltammetric tubes. Also, in order to avoid interference with the previous measuring tools, each electrode was used only once.

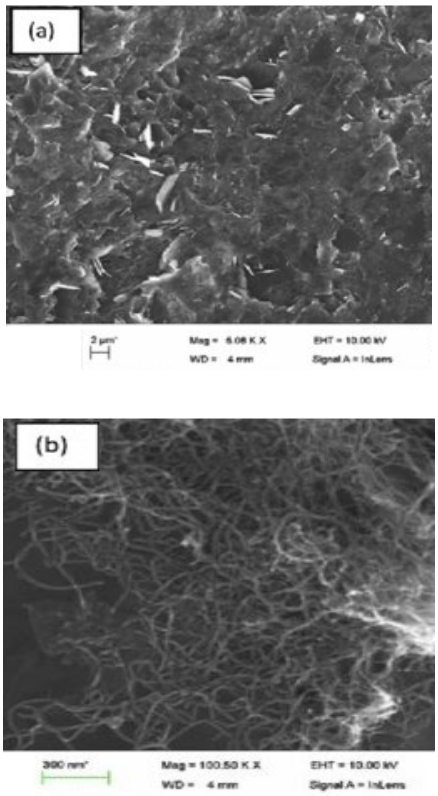

Fig. 2. SEM images of (a) bare PGE, (b) MWCNTs/PGE

2.9. Suggested method procedure

10 mL buffer solution (pH = 6) was transferred to an electrochemical cell of a tri-electrode system, which included a hollow fiber/PGE electrode as a working electrode. Then 5mL of drug sample solutions with appropriate concentrations was added into the buffer solution. A differential pulse voltammograms (DPV) of the analyte in the potential range of 0.0 V to +0.50 V and a frequency of 15 Hz to the 20 mV pulse amplitude was applied, and the peak was recorded as the analyte signal. The calibration curve was plotted based on the current measured relative to the concentration of drugs in the solution. A similar method was used for the blank solution (see Scheme 1).

2.10. Real samples Preparation

2.10.1. Water sample

In order to extract and measure the drugs in water samples, three water samples (drinking water in Bojnourd, Bash Qardash River water and sewage sources in the city of Bojnourd) were selected. At first, the samples were filtered to remove suspended particles, and then, according to the proposed method the target analyte was concentrated and measured. To confirm the validity and applicability of the suggested method for the water sample, certain amounts of standard solutions of lorazepam were added to the water samples and the recommended method was repeated.

2.10.2. Hair sample

The human hair sample which was donated voluntarily was soaked in alcohol in acetone for 40 minutes, washed with water and then dried in an oven. 5.0 g of weighed sample was digested by 20 mL of perchloric acid/nitric acid mixture (with a volume ratio of 8:1).The extract was then evaporated on a water bath to reduce its volume. Eventually, 10 drops of sulfuric acid were added to the residue [33], the solution was transferred to a 100 mL volumetric flask and was brought to volume with deionized water up to the index mark. Then a certain volume of the solution was removed and used to determine the amount of drugs by the proposed method.

3. RESULTS AND DISCUSSION

3.1. Optimization of experimental parameters

3.1.1. Effect of different ILs in optimization process

In order to study the effect of the ILs on the extraction efficiency, different ILs such as: ([BMIM]/[PF_6]),([OMIM][BF_4]), and ([HMIM][PF_6]),were compared. Giving to the data reported in Figure S_6, Fe_3O_4 NPs modified with ([HMIM][PF_6]) had better outcome for lorazepam separation in contrast with the other ILs. The interaction of ionic liquids with the target drug is depending on hydrophobic interactions which can be amplified by π–π interaction, electrostatic interaction, and hydrogen bonding. The ionic species are responsible in the interactions between ILs and Fe_3O_4. But about the interaction between ILs and nanoparticles the imidazolium ring is answerable for interactions with adsorbent and analytes. So, among the mentioned ILs, [HMIM][PF_6] with more reactive anions and longer hydrophobic chains causes the stronger interactions between the nanocomposite and lorazepam. So, this IL was selected for further studies as shown in Scheme 1. The bareFe_3O_4 NPs show a limit adsorption empathy for lorazepam but, when nanomagnetite is preserved with ILs, it obtains good empathy toward target analyte. The fabricated method was stand on the hydrophobic IL adsorption on the surface of nanomagnetite and lead to construction of numerous layers on it. In the same way, the reasonable interactions include dipole–dipole contact and hydrogen bonding with robust sites on the Fe_3O_4 surface is expected. However, chemical sorption of the ionic liquid on the nanostructure surface doesn't happen arbitrarily [35,36].

3.1.2. Screening design

In screening methods, a relatively large number of factors can be studied using a small number of tests and are often used to determine the most influential factors on the response. One of the most common screening methods are the Plackett-Burman design and the Fractional factorial design. However, many factors affect the process of extracting and measuring drug such as the amount of nanoparticles (X1), pH (X2), initial concentration of drugs (X3), deposition time (X4), deposition potential (X5) and scan rate (X6), some of which do not have any significant effect on

it. Therefore, screening factors that are more effective in extracting and measuring analytes is important. In this study, the Plackett-Burman (PBD) surface response method, as a valuable design with a small number of tests, was used to find the more effective factors on the process. Before optimizing the parameters using PBD, the central composite design (CCD) was employed in order to minimize the number of experiments needed for the determination of the best parameters which are effective in the quantitative process. The values, signs and levels of each factor are listed in high levels (+) and lower (-) in Table S1. Twelve experiments were undergone and each experiment was repeated three times, with the average response (current) listed in Table S2 .

The influence of effective factors on the screening tests and the statistical significance, at 95% confidence level (P=0.05), are depicted in Fig. 3 in the Pareto chart.

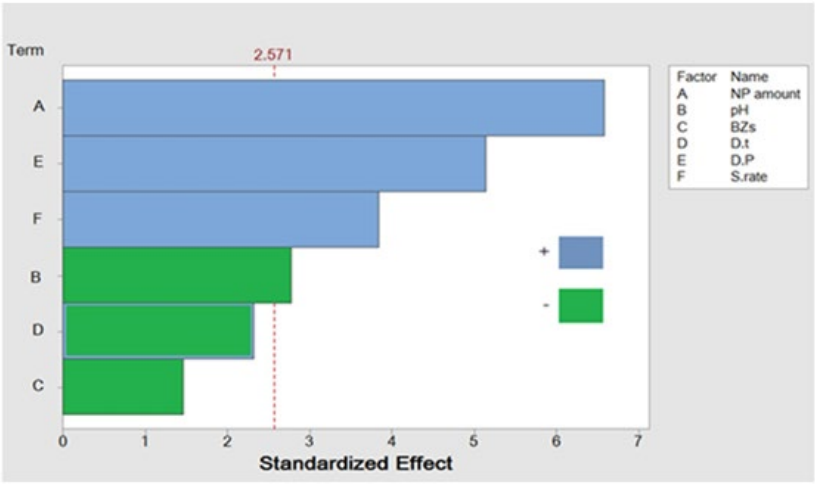

Fig. 3. Pareto chart of the main effects derived from 2-level factorial design for LRZ measurement

Based on Fig. 3, among the tested factors, the amount of nanoparticles, deposition potential, scan rate and pH are the most important factors on the PBD method, and drug concentration and deposition time are less important. It also shows that the drug concentration and the scan rate have the reducing effect on the responses and in contrast, the amount of nanoparticles, scan rate and deposition potential has the positive effects on the responses. Therefore, in order to obtain the exact number of factors that had the greatest effect on the result, they were optimized by the CCD method in 5 levels. According to Fig. 3, the non-effective parameters were fixed in all experiments.

3.1.3. Factors optimization using CCD

Achieving the optimal conditions, usually starts with a screening design to accomplish the most effective factors, so central composite design (CCD) was used for designing this study. We review optimal conditions of each factor and their effect on each other [34].In this study, the CCD has been used, which is one of the response-surface methods. In this method, each

factor is defined at five levels: -1, 0, +1,+α, -α. In this case, the total number of experiments is equal to n_0+k2+ 2^k; where k is the number of independent variables and n_0, the number of replicates of the experiments at the central points. The values of α depend on the number of variables and are calculated on the basis of $\alpha = \pm 2^{f/4}$. Optimum conditions, without the need for the combination of all possible tests, are calculated using the test design based on the response level method. The response behavior is analyzed with a quadratic polynomial. Therefore, using the CCD method and version16 of Minitab software, optimal conditions such as: the amount of nanoparticles (A), pH (B), deposition potential (E) and scan rate (F) were used in five levels to determine the best experimental conditions.

The design consisted of 30 experiments, in which the range of variables was studied based on the previous reported studies in the pH range of2-10, the amount of nanoparticles 5-45 (mg), deposition potential (V) 0.6-0.2 and scan rate of 50-90 (mVS^{-1}). The main factors sign and their levels, and the design of the experiments are shown in Tables 1 and S3, respectively.

Table 1. Factors and levels used in the CCD

Variables	**Levels**					
	Symbols	-α	-1	0	+1	+α
pH	A	2	4	6	8	10
Amount of nanoparticles (mg)	B	5	15	25	35	45
Deposition potential (V)	C	0.2	0.3	0.4	0.5	0.6
Scan rate (mVS^{-1})	D	10	2	70	80	90

To investigate all possible effects of factors including the interaction between the factors and nonlinear relationships with the responses, a complete quadratic model was chosen among the models (Equation 1).

$$y = \beta_0 + \sum \beta_i x_i + \sum \beta_{ii} x_i^2 + \sum \sum \beta_{ij} x_i x_j \qquad (1)$$

Y is Propagation response and $\beta_0, \beta_i, \beta_{ii}$ and β_{ij} are coefficients of calibration model, while x_i,- x_j are real and encoded independent factors. Also, the proposed model was utilized for the analysis using variance ANOVA. The statistical significance of the model was investigated with P value (P-value) and F-value (F value). Statistical tests were performed to determine whether the analyzed factors are statistically significant. The resulting model is as follows (Equation 2).

Current (I) = -36.2 + 1.74 Scan Rate + 4.16 Deposition potential - 0.636NPs amount+ 0.01078 NPs amount×NPs amount- 0.00397 Scan rate×NP amount (2)

The significance of the effect of each parameter or the interaction of the variables is investigated by analysis of variance and F test. The corresponding statistical parameters are shown in Table S4. The quality of the suitability of the polynomial model with the coefficient of determination of R^2 is expressed by the F test. Due to the proximity of R^2 and modified R^2 of the results are consistent with the designed model. One of the parameters used to validate the model's suitability is the lack of a fit parameter shown in Table S4. This parameter is considered as a measure of the degree of in-compatibility of the data to the model. The value of this parameter was 0.860 for the designed model, which is acceptable. The variance analysis was used to evaluate the model (Table S4).

Based on the results of the analysis of variance, F=32.71 indicates that the proposed model is significant for measuring the lorazepam. On the other hand, the value of P is smaller than 0.0001 for the quadratic equation, and shows the statistical significance of the model. Also, the correlation coefficient of the proposed model (R^2=0.9758) is reasonably consistent with the value of the adjusted correlation coefficient (R^2=0.9459). P values less than 0.05 in the ANOVA table indicate the significance of the effect at 95% confidence level. This model, as expressed in Equation 2, consists of three main factors, one two factors and a curve factor. In Equation (2), the positive and negative coefficients of the factors indicate how to change these variables in the response. The absolute value of a factor shows the impact of its affiliates. Variables that have a positive coefficient increase the current of measurement when changing from their lowest value to their highest value. But variables that have a negative coefficient are measured at the time of changing from their lowest value to the highest current. As the above equation indicates, the amount of deposition potential can have the most positive effect on the current of drug measurements. Graphical interpretation of interactions is represented by three-dimensional designs (see Fig. S4).

In this chart, it was generally observed that the scan rate had a more significant effect on drug measurement current compared to pH, and this impact at a pH less than 7 has had a greater slope by increasing the scan rate. According to the results, an increase in pH has a more negative effect on the measured current, so in pH values greater than 7, current drops significantly, without taking into consideration the increase in the potential for deposition.

As illustrated in Fig. S4, an increase in the amount of nanoparticles raises the current, and this increase is more evident in acidic conditions.

Similarly, a simultaneous increase in the deposition potential and the scan rate increases the current. Also, the current rate increases with the simultaneous increase of the scan rate and the amount of nanoparticles.

With the increase of each of the variables i.e., the amount of applied deposition potential and the amount of nanoparticles, the measured current increased.

For investigate the behavior of drug on the designed electrode and to measure it in real samples, the optimal conditions according to the equation obtained from the minitab program was utilized and the interpretation of the interaction of the effective parameters of the three-dimensional charts, parameters A (NPs amount, mg), E (Deposition potential, V) and F (Scan rate, mVS^{-1}) stood at 60 mg, 0.6 V, and 100 mVS^{-1}.

3.2. Voltammetric behavior of Modified and un-modified PGEs

The electrochemical behavior of 100 nM solution of lorazepam at different levels of un-modified PGE, modified PGE with multi-walled carbon nanotube (MWCNTs) and modified hollow fiber modified PGE were investigated using cyclic voltammetry under a potential window of -0.1 V to 0.50 V in phosphate buffer solution 0.1 M (pH 6) and under optimum conditions (60.0 mg adsorbent, 0.6 V deposition potential and 100 mV s^{-1}scan rate).

The results showed that lorazepam had a reduction peak at +0.28V compared to silver-silver chloride reference electrode. As shown in Fig. S5, at the un-modified electrode surface, a very poor response was obtained for the oxidation of lorazepam. While at the levels of PGE modified with magnetic multi-walled carbon nanotube and modified pencil graphite with enhanced hallow fiber, there was a significant improvement in the target analyte oxidation peak. In addition, the modified pencil graphite electrode along with the strengthened hallow fiber the current was more significant. That indicates the positive effect of magnetic multi-walled carbon nanotube and ionic liquid in improving the response. This increase of voltammetric response can be attributed to the effective adsorption of lorazepam by ionic liquid and magnetite MWCNTs. Therefore, after an investigation on the electrophiliicity of lorazepam on the provided electrode, this electrode was used for further studies. Also, as for the high sensitivity of the derivative pulsed voltammetry, the proposed method was used to determine and measure lorazepam, quantitatively.

3.2.1. Electrochemical characterization

Cyclic voltammetry with different potential sweep rates was used to determine the effect of scan rate on the lorazepam oxidation peak. The electrochemical characteristics in the stepwise fabrication process of the HF-PGE were studied by cyclic voltammetry (CV) with 1.0 mmol L^{-1} $[Fe(CN)_6]^{3-}/[Fe(CN)_6]^{4-}$ containing 0.1 mol L^{-1} KCl probe solution.

Fig. 4 shows a typical comparison of cyclic voltammograms of the bare PGE, and MWCNTs/IL/HF-PGE. Compared to the bare PGE (Fig. 4a), the peak current of the PGE which was modified with MWCNTs/IL nanocomposite increases and the redox peak separation (ΔE_p) decreases (Fig. 4b).

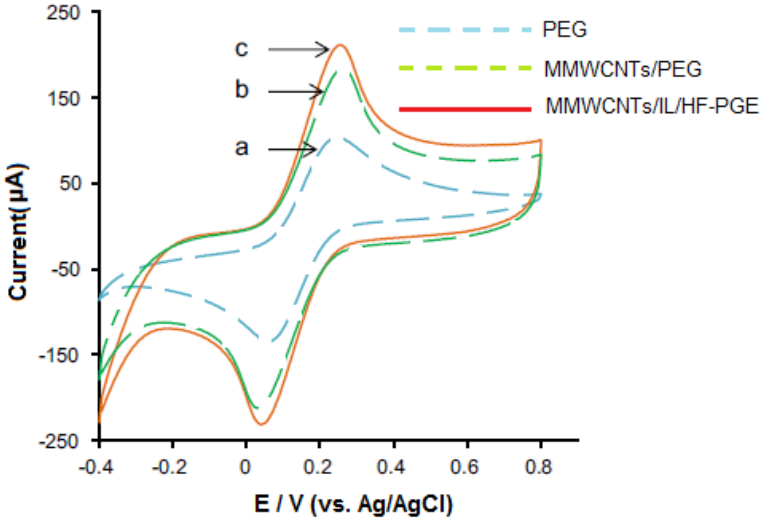

Fig. 4. Cyclic voltammograms of (a) Bare PGE, (b) MMWCNTs/IL/HF-PGE in 1.0 mmol L^{-1} $[Fe(CN)_6]^{3-}/[Fe(CN)_6]^{4-}$ containing 0.1 mol L^{-1} KCl probe solution

On the other hand, when the MWCNTs/IL nanocomposite modified PGE was placed inside the lumen of the hollow fiber while its wall pores are filled with MWCNTs/IL, the highest redox peak current and lower background current was observed (Fig. 4c). This was probably because the MWCNTs/IL nanocomposite could effectively increase surface area and active sites of the electrode and IL could enhance the electrical conductivity of the composite materials.

The active surface areas of the bare PGE, MWCNTs/PGE and MWCNTs/IL/HF-PGE were calculated using the Randles–Sevcik Equation (3):

$$I_{pa} = (2.69 \times 10^{5})\, n^{3/2}.\, A_0.\, D_0^{1/2}.\, C_0.\, v^{1/2} \qquad (3)$$

where I_{pa} refers to the anodic peak current, n is the number of electrons transferred, A_0 is the surface area of the electrode, D_0 is diffusion coefficient, v is the scan rate and C_0 is the concentration of the probe molecule. For 1.0 mmol L^{-1} $[Fe(CN)_6]^{3-/4-}$ in 0.1 mol L^{-1} KCl electrolyte, n=1, $D_0=1.8\times10^{-6}$ cm^2 s^{-1}, then from the slope of the plot of I_{pa} *vs.* $v^{1/2}$, the electroactive area was calculated. In our experiment the area of electrodes was calculated and the values are as follows; 0.160, 0.201 and 0.236 cm^2 for PGE, MWCNTs/PGE and MWCNTs/IL/HF-PEG respectively. This results clearly show that MWCNTs/IL nanocomposite greatly enhance the effective surface area of the modified electrode.

According to the Randles-Sevcik equation, for a linear diffusion controlled process, I_p is proportional to $v^{1/2}$, and for the adsorptive process, I_{pis} proportional to v. Experimental results indicated that when the scan rate is increased from 20 to 500 mV/s at a fixed concentration of lorazepam, the peak potential shifted to a more positive potential and the peak current increased steadily. The anodic peak currents were linear with the square root of scan rate as

shown in Equation 5 (Fig. 5A), The dependence of peak current (I_p) on the scan rate (v) as shown in Fig. 5B, indicates that I_p increases with increasing scan rate($v^{1/2}$), which may be expressed by Equation 4:

$$I\ (\mu A) = 2.5836v^{1/2} – 2.0996\ R^2 = 0.9971 \quad (4)$$

$$I\ (\mu A) = 0.1225v\ -0.2979\ R^2 = 0.9928 \quad (5)$$

These results indicated that the electrochemical behavior of lorazepam on the magnetic multi-walled carbon nanotube-ionic liquid composite on a Hollow Fiber-Pencil Graphite Electrode is a diffusion-controlled process.

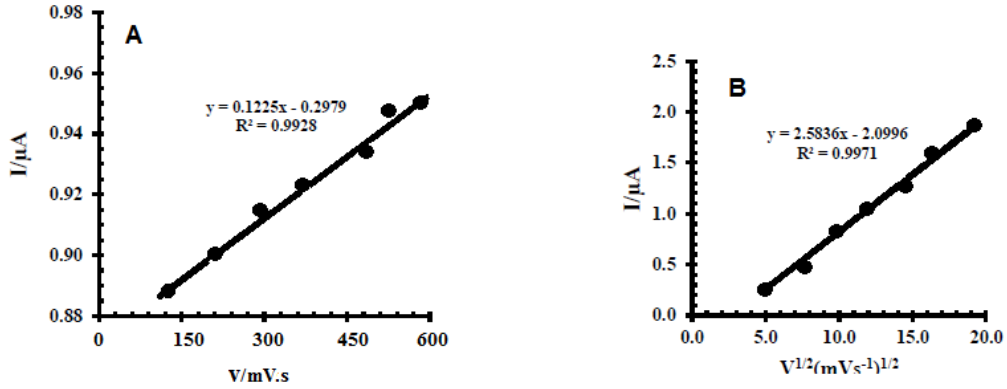

Fig. 5. Plots of (A) I_p versus v and (B) I_p *vs.* $v^{1/2}$ at the magnetic multi-walled carbon nanotube-ionic liquid composite on a Hollow Fiber-Pencil Graphite Electrode

3.2.1. Method performance assessment

In assessing any analytical method, the method eligibility criteria are very important. The dynamic range, detection limit and limit of quantification, repeatability and selectivity are among the method eligibility criteria. The analytical methods should be repeatable, have a large linear range plus low detection limits and should be able to be used to analyze the real samples.

3.2.2. Calibration curve and statistical analysis

In order to plot the calibration curve and determine the linear range of the present method, aqueous solutions were prepared with different concentrations of lorazepam, extracted and preconcentrated according to the mentioned method and then the samples simultaneously were measured by a voltammetric device.

As shown in Fig. 6, there is linearity between the current and concentration of standards in the concentration range of 0.1-200 nM of lorazepam.

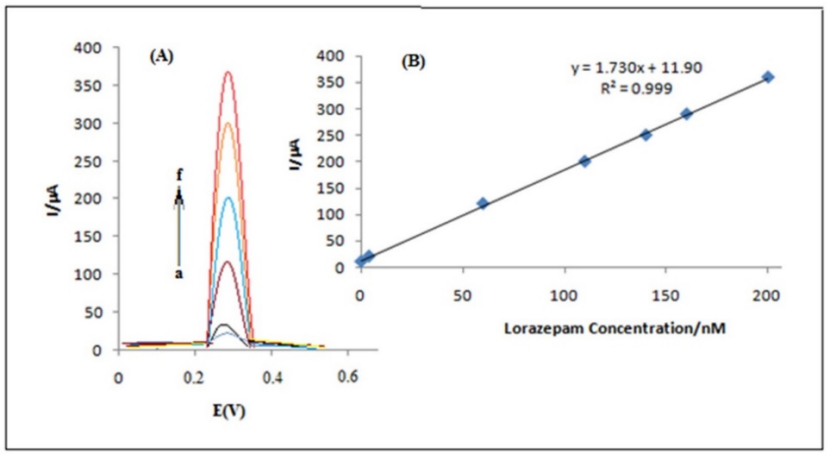

Fig. 6. (A) Lorazapam-differential pulse voltammograms in phosphate buffer pH = 6 at a concentration of (a-f): 0.1, 5, 60, 110, 140, 160 and 200 nM. (B) Linear calibration curve of the anodic peak current according to the concentration of lorazepam

The limit of detection (LOD) and quantification (LOQ) was detected, using the expression; kS_b/m, where S_b is the standard deviation of blank measurement (N=5) and, m is the slope of the calibration curve, statistical k factor is equal to 3 for LOD and equal to 10 for LOQ. The calculated values for LOD and LOQ are 0.003 μM and 0.06 μM, respectively. In addition, for 3 repeated measurements of the lorazepam standard solutions under optimal conditions, a good repeatability with a standard deviation of 3.48% was obtained.

Table 2 displays the qualities of the suggested method compared to other researches in this field.

Table 2. Comparison between the proposed method and other methods

Method	Analyte	LDR*	R^2	LOD	LOQ	R%	Ref.
SPE-UPLC-MS-MS	LRZ	2-500	0.993	0.05	2	88.7	[37]
LLE-EI-GC-MS	LRZ	50-400	0.9999	3.89	11.8	90.0	[38]
LL/SPE-HPLC-UV	LRZ	50-1200	0.9973	20	50	90.2	[39]
D-μ-SPE[a]-HPLC-UV	LRZ	5-2000	0.995	1.8	5.0	90.0	[40]
HF-SLPME	LRZ	0.032-64.2	0.995	0.003	0.060	98.0	This work

*All concentrations are based on μg L^{-1}
[a] Dispersive micro-solid phase extraction
[b] Hollow fiber-solid liquid phase microextraction

3.2.3. Effect of interferences

To assess the efficiency of the synthesized electrode, the interfering effect of different types of molecules on the determination of lorazepam was assessed and investigated. The selectivity of this electrode was measured in a concentration of 50.0 μM of lorazepam by adding more concentrations of some of the interfering species by voltammetric method. The

interruption limit was considered at the concentration that the interfering species caused a change in the analyte signal to more than 5% of the initial value. If the potential and current changes are not higher than 5%, then the presence of that substance can be considered as a non- interfering species.

The results (Table 3) show that these compounds at relevant concentrations do not significantly interfere with the voltammetric measurement of lorazepam.

3.2.4. The applicability of the fabricated electrode to real samples

In order to investigate the ability of the proposed electrode to analyze the real samples, the presence of lorazepam in domestic water, urine and hair samples was studied according to suggested method.

Table 3. The effect of different interferences on the voltammetric response of lorazepam

Interfering Molecule	**Concentration of interference (µM)**	**LRZ Response change[a] ± SD (µA)**	**Signal change (%)**
Ascorbic acid	100	+ 0.041 ± 0.001	3.10
	200	+ 0.045 ± 0.002	3.22
	500	+ 0.047 ± 0.001	3.50
	1000	+ 0.051 ± 0.003	3.80
	2000	+ 0.530 ± 0.001	4.51
Glucose	100	+ 0.050 ± 0.002	3.77
	200	+ 0.052 ± 0.001	4.11
	500	+ 0.053 ± 0.004	4.50
	1000	+ 0.057 ± 0.003	4.55
	2000	+ 0.063 ± 0.001	4.80
Uric acid	100	+ 0.022 ± 0.001	2.33
	200	+ 0.032 ± 0.001	2.74
	500	+ 0.041± 0.002	3.21
	100	+ 0.044 ± 0.005	3.48
	2000	+ 0.049 ± 0.002	3.99
Urea	100	+ 0.030 ± 0.001	2.71
	200	+ 0.039 ± 0.002	2.93
	500	+ 0.043 ± 0.001	3.34
	100	+ 0.049 ± 0.004	3.70
	2000	+ 0.052 ± 0.002	3.93

[a]The Concentration of LRZ=50 µM in all experiments and in the absence of any interference the current was 1.96 µA

The results, along with relative recoveries, have been reported in Table 4, which indicates the accuracy and applicability of the method for extracting and determining lorazepam.

Table 4. Measurement of lorazepam in real samples (n = 5)

Sample	Concentration of Lorazepam (μM) [(a)]		RR%[(b)]	RSD%
	Added	Found± RSD[a]		
River water	-	0.0	-	-
	10	10.2±0.01	102.0	1.8
	20	20.4±0.02	101.0	2.8
	30	29.4±0.03	99.0	3.2
Urine	-	0.0	-	-
	10	10.23±0.002	102.8	2.4
	20	20.14±0.003	101.1	1.9
	30	30.26±0.006	101.2	3.2
Hair	-	82.6±0.006	-	3.1
	20	103.2±0.003	100.2	4.2
	30	113.1±0.004	100.2	2.3

[(a)]Mean average of five determinations, (b) Relative recovery percent

4. CONCLUSION

In this study, the combination of hollow fiber supported nanoparticles and an ionic liquid in the form of a new electrochemical sensor was used to measure trace amounts of lorazepam. The use of ionic liquids as an effective agent in hollow fiber cavities resulted in good pre-concentration of benzodiazepine drug. In addition, the using of multi-walled carbon nanoparticles to modify the surface of pencil graphite electrode showed an increase in electron transfer rate at the electrode surface, which in turn reduced the overvoltage and increased the sensitivity of the method. The prepared electrode showed significant advantages such as, acceptable accuracy and precision, wide linear dynamic range and a low detection limit. Moreover, the simplicity of the equipment used, was an extra advantage of this method. The results of electrochemical studies showed (Fig. S5) that the surface area of the electro-active agent increased thereby significantly increasing the lorazepam current peak. Therefore, this electrode was successfully used to measure lorazepam in real samples.

REFERENCES

[1] C. Page, B. Hoffman, M. Curtis, and M. Walker, Integrated Pharmacology: With Student Consult Access, 3rd Ed., Michael JA Walker, London (2006).

[2] A. S. Lippa, J. Coupet, E. N. Greenblatt, C. A. Klepner, and B. Beer, Pharmacol. Biochem. Behav. 11 (1979) 99.

[3] K. T. Olkkola, and J. Ahonen, Midazolam and other benzodiazepines, Modern anesthetics, Springer, Berlin, Heidelberg (2008).

[4] K. R. Tan, U. Rudolph, and C. Lüscher, Trends Neurosci. 34 (2011) 188.

[5] J. Riss, J. Cloyd, J. Gates, and S. Collins, Acta Neurol. Scand. 118 (2008) 69.
[6] C. M. Kahn, L. Scott, and S. E. Aiello, The Merck veterinary manual, 9th ed., Philadelphia, Pensylvania (2005).
[7] A. Bugey, and C. Staub, J. Pharm. Biomed. Anal. 35 (2004) 555.
[8] E. Bertol, F. Vaiano, M. Borsotti, M. Quercioli, and F. Mari, J. Anal. Toxicol 37 (2013) 659.
[9] V. F. Samanidou, M. N. Uddin, and I. N. Papadoyannis, Bioanalysis 1 (2009) 775.
[10] D. Borrey, E. Meyer, W. Lambert, S. Van Peteghem, C. Van Peteghem, and A. P. DeLeenheer, J. Chromatogr. A 910 (2001) 105.
[11] K. Arnhard, R. Schmid, U. Kobold, and R. Thiele, Anal. Bioanal. Chem. 403 (2012) 755.
[12] P. Adamowicz, and M. Kała, Forensic Sci. Int. 198 (2010) 39.
[13] D. R. Baker, and B. Kasprzyk-Hordern, J. Chromatogr. A 1218 (2011) 1620.
[14] M. Huerta-Fontela, M. T. Galcerán, and F. Ventura, J. Chromatogr. A 1217 (2010) 4212.
[15] S. Esteban, Y. Valcárcel, M. Catalá, and M. G. Castromil, Gac Sanit 26 (2012) 457.
[16] A. Mendoza, M. López de Alda, S. González-Alonso, N. Mastroianni, D. Barceló, and Y. Valcárcel, Chemosphere 95 (2014) 247.
[17] A. Jurado, N. Mastroianni, E. Vàzquez-Su˜né, J. Carrera, I. Tubau, E. Pujades, C. Postigo, M. López de Alda, and D. Barceló, Sci. Total Environ. 424 (2012) 280.
[18] C. Repice, M. Dal Grande, R. Maggi, and R. Pedrazzani, Sci. Total Environ. 27 (2013) 463.
[19] F. T. Peters, Clin. Biochem. 44 (2011) 54.
[20] A. Salomone, E. Gerace, P. Brizio, M. C. Gennaro, and M. Vincenti, J. Pharm Anal. 56 (2011) 582.
[21] H. H. Lee, J. F. Lee, S. Y. Lin, Y. Y. Lin, C. F. Wu, M. T. Wu, and B. H. Chen, Clin. Chim. Acta 420 (2013) 134.
[22] K. Wang, M. Cheng, C. Hsieh, J. Hsu, J. Wu, and C. Lee, Forensic Sci. Int. 224 (2013) 84.
[23] X. P. Lee, T. Kumazawa, J. Sato, Y. Shoji, C. Hasegawa, C. Karibe, T. Arinobu, H. Seno, and K. Sato, Anal. Chim. Acta. 492 (2003) 223.
[24] L. M. de Carvalho, D. Correia, S. C. Garcia, A.V. de Bairros, P. C. d. Nascimento, and D. Bohrer, Forensic Sci. Int. 202 (2010) 75.
[25] K. B. Borges, E. F. Freire, I. Martins, and M. E. P. B. de Siqueira, Talanta 78 (2009) 233.
[26] R. A. Anderson, M. M. Ariffin, P. A. G. Cormack, and E. I. Miller, Forensic Sci. Int.174 (2008) 40.

[27] K. Johansen Reubsaet, H. Ragnar Norli, P. Hemmersbach, and K. E. Rasmussen, J. Pharm. Biomed. Anal. 18 (1998) 667.
[28] H. G. Ugland, M. Krogh, and L. Reubsaet, J. Chromatogr. B 798 (2003) 127.
[29] Z. Es'haghi, A. Nezhadali, S. Bahar, S. Bohlooli, and A. Banaei, J. Chromatogr. B 980 (2015) 55.
[30] Z. Es'haghia, M. Ahmadi-Golsefidi, A. Saify, A. A. Tanha, Z. Rezaeifar, and Z. Alian-Nezhadi, J. Chromatogr. A 1217 (2010) 2768.
[31] X. Huang, L. Chen, D. Yuan, and S. Bi, J. Chromatogr. A 1248 (2012) 67.
[32] S. Wu, A. Sun, F. Zhai, J. Wang, W. Xu, Q. Zhang, and A. Volinsky, Mater. Lett. 65 (2011) 1882.
[33] L. Jiaming, L. Xuana, W. Aihong, H. Li-Xiang, H. E. Hangxia, H. Honghua, L. Longdi, and L. Shaoqin, Spectrochim. Acta A Mol. Biomol. Spectrosc. 65 (2006) 106.
[34] K. M. Sharif, M. M. Rahman, J. Azmir, A. Mohamed, M. H. A. Jahurul, F. Sahena, and I. S. M. Zaidul, J. Food Eng. 124 (2014) 105.
[35] M. Bayat, F. Shemirani, M. Hossein Beyki, and M. Davudabadi Farahani, Desalination Water Treat 56 (2015) 814.
[36] R. Verplaetse, E. Cuypers, and J. Tytgat, J. Chromatogr. A 1249 (2012) 147.
[37] M. D. Bermúdez, A. E. Jiménez, J. Sanes, and F. J, Carrión, Molecules 14 (2009) 2888.
[38] I. I. Papoutsis, S. A. Athanaselis, P. D. Nikolaou, C. M. Pistos, C. A. Spiliopoulou, and C. P. Maravelias, J. Pharm. Biomed. Anal. 52 (2010) 609.
[39] K. B. Borges, E. F. Freire, I. Martins and M. E. P. B. De Siqueira, Talanta 78 (2009) 233.
[40] A. A. Asgharinezhad, H. Ebrahimzadeh, F. Mirbabaei, N. Mollazadeh, and N. Shekari, Anal. Chim. Acta. 844 (2014) 80.